SLEEP-MODULATED PATHWAYS IN NEUROPROTECTION FROM STROKE

Identification of Sleep-Modulated Pathways Involved in Neuroprotection from Stroke

Marta Pace, MSc[1,2,*]; Francesca Baracchi, PhD[1,*]; Bo Gao, MD[1]; Claudio Bassetti, MD[1,2]

*[1]ZEN – Zentrum für Experimentelle Neurologie, Inselspital, Bern, Switzerland; [2]Graduate School for Cellular and Biomedical Sciences, University of Bern, Bern, Switzerland; *co-first authors*

Study Objectives: Sleep deprivation (SDp) performed before stroke induces an ischemic tolerance state as observed in other forms of preconditioning. As the mechanisms underlying this effect are not well understood, we used DNA oligonucleotide microarray analysis to identify the genes and the gene-pathways underlying SDp preconditioning effects.

Design: Gene expression was analyzed 3 days after stroke in 4 experimental groups: (i) SDp performed before focal cerebral ischemia (IS) induction; (ii) SDp performed before sham surgery; (iii) IS without SDp; and (iv) sham surgery without SDp. SDp was performed by gentle handling during the last 6 h of the light period, and ischemia was induced immediately after.

Settings: Basic sleep research laboratory.

Measurements and Results: Stroke induced a massive alteration in gene expression both in sleep deprived and non-sleep deprived animals. However, compared to animals that underwent ischemia alone, SDp induced a general reduction in transcriptional changes with a reduction in the upregulation of genes involved in cell cycle regulation and immune response. Moreover, an upregulation of a new neuroendocrine pathway which included melanin concentrating hormone, glycoprotein hormones-α-polypeptide and hypocretin was observed exclusively in rats sleep deprived before stroke.

Conclusion: Our data indicate that sleep deprivation before stroke reprogrammed the signaling response to injury. The inhibition of cell cycle regulation and inflammation are neuroprotective mechanisms reported also for other forms of preconditioning treatment, whereas the implication of the neuroendocrine function is novel and has never been described before. These results therefore provide new insights into neuroprotective mechanisms involved in ischemic tolerance mechanisms.

Keywords: stroke, sleep deprivation, preconditioning, neuroprotection

Citation: Pace M, Baracchi F, Gao B, Bassetti C. Identification of sleep-modulated pathways involved in neuroprotection from stroke. *SLEEP* 2015;38(11):1707–1718.

INTRODUCTION

Despite recent progress in the understanding of pathways involved in neuronal damage during stroke, limited advances have been achieved in developing therapies to limit ischemia. Reperfusion therapy remains the only approved treatment, and it is delivered in fewer than 10% of admitted patients due to the narrow therapeutic window and safety concern.[1] This emphasizes the need for alternative therapies that can enhance neuroprotection by antagonizing the molecular cascades underlying cellular damage and mortality.

In the last few years, both clinical and preclinical settings suggested a beneficial role for sleep on stroke recovery. Indeed, it has been established that not only do sleep disorders contribute to stroke vascular pathology,[2] but that sleep alterations following stroke are usually linked with poorer rehabilitation and long-term outcomes.[3] Recent studies on animal models clearly showed that increasing length and repetition of sleep deprivation (SDp) during the acute phase of ischemia has detrimental effects, both on stroke evolution and functional recovery.[4,5] In contrast, the pharmacological enhancement of sleep after stroke has been linked with faster behavioral recovery in mice,[6] as well as axonal sprouting and neurogenesis in rats.[7] We and others have shown that SDp protocols prior to an experimentally induced stroke did not have a detrimental impact on recovery, but instead induced a protective effect on the brain, resulting in a reduction of the neuronal damage 7 days after stroke with a concomitant improvement in the recovery of sensorimotor performance and motor coordination.[8–11] Since these beneficial effects were associated also to a reduction in post-stroke inflammatory response,[8,9] SDp prior to stroke has been compared to a phenomenon known as ischemic tolerance, or *preconditioning*. This phenomenon has been described in the literature for several type of stimuli (hypothermia, hypoxia, oxidative stress, and others) and it is defined as *the application of a potentially harmful stimulus, near to but below the threshold of cell damage, which promotes the tolerance of the brain to subsequent ischemic injury.*[12] Although the mechanisms underlying this tolerance remain unclear, a reduction in the post-stroke inflammatory response, which is considered to contribute to ischemic brain injury, seems to be a common pathway in other forms of preconditioning.[13] However, since sleep is involved in the central and peripheral modulation of many molecular functions,[14,15] some of which also involved in stroke pathophysiology,[12,16] other pathways such as energy balance,[17–19] thermoregulation,[20,21] or anti-oxidant systems[22,23] might play a role in the ischemic tolerance induced by SDp. The aim of this study was to investigate which are the mechanisms and the pathways involved in neuroprotection induced by pre-stroke SDp, in

A commentary on this article appears in this issue on page 1671.

Submitted for publication January, 2015
Submitted in final revised form March, 2015
Accepted for publication April, 2015

Address correspondence to: Francesca Baracchi, PhD, ZEN - Zentrum für Experimentelle Neurologie, Department of Neurology, Inselspital, Bern University Hospital, Freiburgstrasse 18, 3010 Bern, Switzerland; Tel: +41 (0)31 63 233 385; Email: francesca.baracchi@gmail.com

order to identify functional and molecular targets for future therapeutic approaches. We therefore performed a microarray study to characterize brain gene expression alterations in rats sleep deprived prior to cerebral ischemia. Moreover based on microarray results we decided to further investigate the peripheral effects of a newly identified pathway so to elucidate its possible role in neuroprotection.

METHODS

Animals

Male Sprague-Dawley rats (n = 24), 8–10 weeks old and weighing 296 ± 35 g at the time of surgery, were used in this study. They were housed under a 12 h light/dark cycle (light on 08:00–20:00) with ambient temperature at 22 ± 0.5°C. Animals were provided ad libitum with food and water except for the 18 h preceding stroke surgery, during which they were food deprived.[10] All experiments were conducted according to local guidelines with governmental approval (Kantonales Veterinäramt Zürich, Switzerland) for the care and use of laboratory animals.

Experimental Design

Rats were assigned to 4 experimental groups: (i) sleep deprivation followed by ischemia (SDp.IS); (ii) sleep deprivation followed by sham surgery (SDp); (iii) ischemia (IS); and (iv) sham surgery (Sham). SDp was performed by gentle handling during the last 6 h of the dark period, and ischemia/sham surgery was performed immediately after. Sixteen rats (n = 4/group) were sacrificed 3 days after surgery. Eight additional rats, assigned to SDp.IS and IS group (n = 4/group), were instead sacrificed after 7 days. Focal cerebral ischemia was induced by electrocoagulation of the distal middle cerebral artery (MCA) and permanent ligation of the ipsilateral common carotid artery (CCA), associated with temporary occlusion (60 min) of the contralateral CCA as previously described.[5,11,24] Sham-control animals were subjected to the same procedure except for the occlusion of the MCA and CCAs. At the end of the protocol, blood was collected before sacrifice and brains were extracted for molecular analysis and ischemic damage evaluation.

Microarray analysis was performed only in rats sacrificed after 3 days, on tissue obtained from the whole ischemic hemisphere. Quantitative Real-time PCR (qRT-PCR) and enzyme-linked immunoassays (ELISA) were performed for animals sacrificed both at 3 and 7 days.

Infarct Volume Evaluation

Rats were decapitated while deeply anesthetized (Isoflurane 5%) and brains dissected and frozen immediately on dry ice; 20 μm coronal sections were cut on a cryostat at 6 predefined levels with 1 mm interval (L-1: 2.7 mm; L-2: 1.7 mm; L-3: 0.7 mm; L-4: −0.3 mm; L-5: −1.3 mm and L-6: −2.3 mm from bregma[24,25]). Twenty sections at each level were mounted on SuperFrostr Plus slides (Menzel GmbH, Braunschweig, Germany) for histology. The remaining tissue between these sections was cut at 50 μm and hemispheres collected separately. Sections were then stored at −80°C for further molecular biology analysis. To determine the volume of the lesion, one section for each level was stained with cresyl violet and digitized. The infarct area was measured at each level by ImageJ software (NIH, Bethesda, MD, USA). The volume was assessed by converting with the known distance between each levels and eventually correcting for edema by multiplying the ratio of the contralateral to ipsilateral volume as described.[26]

Microarray Analysis

RNA was isolated separately from ipsilateral and contralateral hemisphere from the 50 μm sections by means of TRIzol/tissue (Sigma Aldrich, Midtown-St Louis, MO, USA) according to manufacturer's instruction.[27] RNA concentration was then determined by a NanoDrop 2000c spectrophotometer.

Quantities of 100 ng of RNA per sample from the ischemic hemisphere were independently used to perform the target preparation using the whole transcript sense target labeling protocol procedure (Affymetrix, High Wycombe, UK). Then, 2.5 μg of each fragmented cDNA was end labeled with biotin and hybridized to a GeneChip Rat Gene 1.0 ST array (Affymetrix). Normalized expression signals for each animal were calculated from Affymetrix CEL files using RMA normalization method implemented in the Affymetrix Expression Console software, version 1.1. 2800. Statistical analyses were performed using the R language, version 2.14.2. P values were adjusted for multiple testing with the Benjamini and Hochberg method.

We fitted a model with a coefficient for each of the 4 factor combinations (IS, SDp, SDp.IS, Sham) and extracted the comparisons of interest as contrasts. Four total contrasts were performed: (1) IS versus Sham (IS/vs/Sham), to evaluate the alterations in gene expression induced by ischemia; (2) SDp.IS versus SDp (SDp.IS/vs/SDp), to evaluate the changes induced by ischemia while controlling possible SDp effects; (3) SDp versus Sham (SDp/vs/Sham), to assess gene alterations induced by SDp alone; and (4) SDp.IS versus IS (SDp.IS/vs/IS), to evaluate the effects of SDp on ischemia. Following MAA-NOVA analyses of all data for each condition, we identified the significantly differentially expressed genes (adjusted qVal cutoff criteria ≤ 0.05). An initial hierarchical clustering analysis was performed to evaluate the segregation of the different samples according to treatment. One animal in the SDp.IS group clustered with sham treated groups and for this reason it was discarded from all subsequent analysis. Due to an unclear separation, 3 other samples (2 SDp and 1 Sham) were excluded from all microarray analysis but included in the following qRT-PCR study as the values of the genes examined were in line with the group mean value.

Data were further analyzed by Ingenuity Pathway Analysis (IPA) Software (Qiagen, Redwood City, CA). Two types of analysis were performed in IPA: the downstream effects analysis (DEA) and functional network generation. DEA was performed in IPA in order to identify biological functions and canonical pathways which were relevant for each contrast. For each biological function, in addition to the P value, another statistical quantity, *activation z-score,* was computed to infer the state of activation of specific functional annotations associated with a particular biological function. A z-score ≥ 2 predicts "increased activation" whereas a z-score ≤ 2 predicts "decreased activation." The generation of functional networks was performed only for the SDp.IS/vs/IS contrast.

Quantitative Real-Time PCR

To validate microarray results we examined the expression of 18 genes (Table S1, supplemental material) by quantitative Real-Time PCR (qRT-PCR) using TaqMan Gene Expression Assay (Life Technologies, Carlsbad, CA, USA). Genes were selected within the functional networks identified for the SDp.IS/vs/IS contrast on the basis of P value and difference in fold change. cDNA for qRT-PCR was obtained from up to 2 μg of total RNA by using a high-capacity RNA-to-cDNA kit (Life Technologies, Carlsbad, CA, USA) and stored at −20°C. qRT-PCR was performed in rats sacrificed at 3 days on both hemispheres and in rats sacrificed at 7 days exclusively on ipsilateral hemisphere.

ELISA Immunoassays

After sampling, blood was centrifuged at 10,000 rpm for 10 min at 4°C to separate the serum. Serum was then stored at −80°C for further use. ELISA immunoassays were performed using kits for testosterone and 17β-estradiol (Abnova, Taipei City, Taiwan) following the manufacturer's protocol.

Statistics

Results of infarct volume, qRT-PCR and ELISA are presented as means ± SD. Differences in lesion volume were assessed by means of t-test for independent samples. qRT-PCR data at day 3 were analyzed by 2-way ANOVA (factors: group and hemisphere), whereas qRT-PCR data comparisons between day 3 and day 7 were analyzed by 1-way ANOVA. ELISA data were also tested by a 2-way ANOVA (factors: group and day). Whenever statistical significant was achieved, post hoc contrasts with Tukey correction were run separately for each factor.

RESULTS

Infarct Volume

In order to confirm the neuroprotective effect of pre-stroke SDp, infarct size was evaluated in both IS and SDp.IS groups 3 and 7 days after stroke. After 7 days, the infarct lesion was significantly smaller in animals which were sleep deprived prior to stroke compared to animals which underwent ischemia without sleep deprivation (SDp.IS: 25.6 ± 7.5 vs IS: 54.4 ± 14.0 mm^3; t-test $P \leq 0.008$). No significant difference between the 2 experimental groups was observed in rats sacrificed after 3 days (IS: 93.7 ± 16.1 vs SDp.IS: 97.2 ± 28.7 mm^3).

Gene Expression Data

As described in the Methods, microarray analysis was performed on 4 different contrasts in order to evaluate separately the effects of the 2 treatments (ischemia and SDp) and also their possible interactions. Contrast 1 (IS/vs/Sham) showed that ischemia altered significantly (adj. $P \leq 0.05$) the expression of 9,303 genes and in particular induced a downregulation of 5,141 genes and an upregulation of 4,162 (Figure 1A). In contrast 2 (SDp.IS/vs/SDp), the number of genes affected by ischemia was lower (7,154; 3,868 downregulated and 3,286 upregulated), indicating a possible interaction between ischemia and SDp effect (Figure 1A). SDp alone (contrast 3) induced an alteration in the expression of 941 genes, of which 401 were downregulated and 540 upregulated (Figure 1A). This was different from what we observed in contrast 4 (SDp.IS/vs/IS) since the effect of SDp induced significant changes in a lower number of genes (820) with a predominant downregulation (555 genes downregulated vs 265 upregulated), indicating an interaction between ischemia and SDp (Figure 1A).

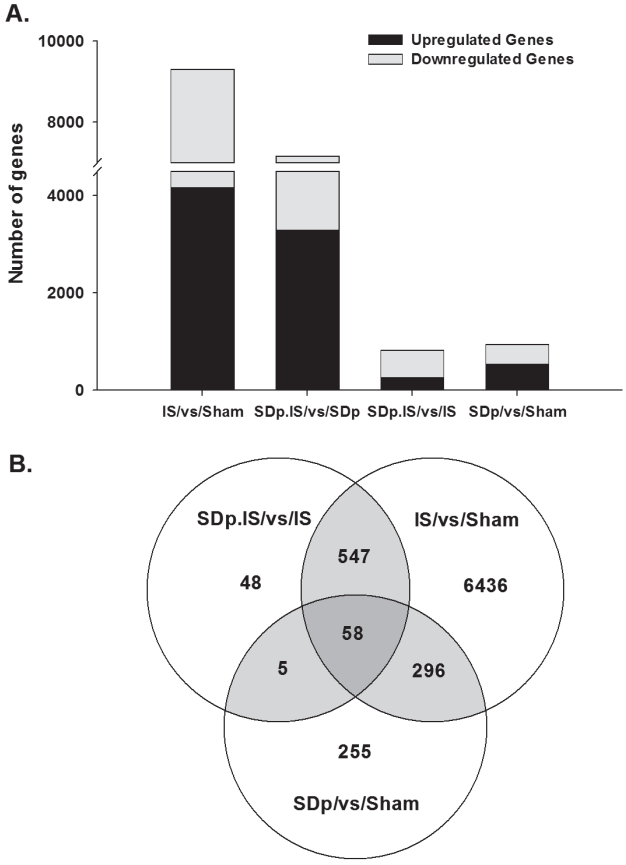

Figure 1—(A) Total number of genes significantly altered (adj. $P \leq 0.05$) in each of the 4 contrasts investigated (IS/vs/Sham; SDp.IS/vs/SDp; SDp/vs/Sham; SDp.IS/vs/IS). Black bars indicate the number of genes which were upregulated; gray bars indicate the number of genes which were downregulated. **(B)** Venn diagram showing the numbers of the common and exclusively expressed genes in the 3 different contrasts: a. IS/vs/Sham; b. SDp/vs/Sham; and c. SDp.IS/vs/IS. Only the identified genes were included in this analysis.

The interaction between treatments was further analyzed in a Venn diagram (Figure 1B) including contrast 1 (IS/vs/Sham), 3 (SDp/vs/Sham), and 4 (SDp.IS/vs/IS). The expression of 6,436 genes (60% upregulated; 40% downregulated) was altered exclusively in the IS/vs/Sham contrast. Of the 547 genes shared between contrast 1 and contrast 4, almost 100% (545 out of 547 genes) showed an opposite regulation in the 2 contrasts, and in particular 80.6% was downregulated in SDp.IS/vs/IS and upregulated in IS/vs/Sham (Table S1). This suggests that the upregulation of these genes induced by IS is actually inhibited by pre-stroke SDp. Fifty-eight genes were found to be common to the 3 contrasts. Compared to the expression in SDp.IS/vs/IS contrast most of these genes (98.3%) showed again an opposite regulation in IS/vs/Sham contrast; only 32.7% were oppositely regulated in the SDp/vs/Sham contrast (Table S2, supplemental material). Forty-eight genes were identified to be altered exclusively in the SDp.IS/vs/IS contrast (Table S3, supplemental

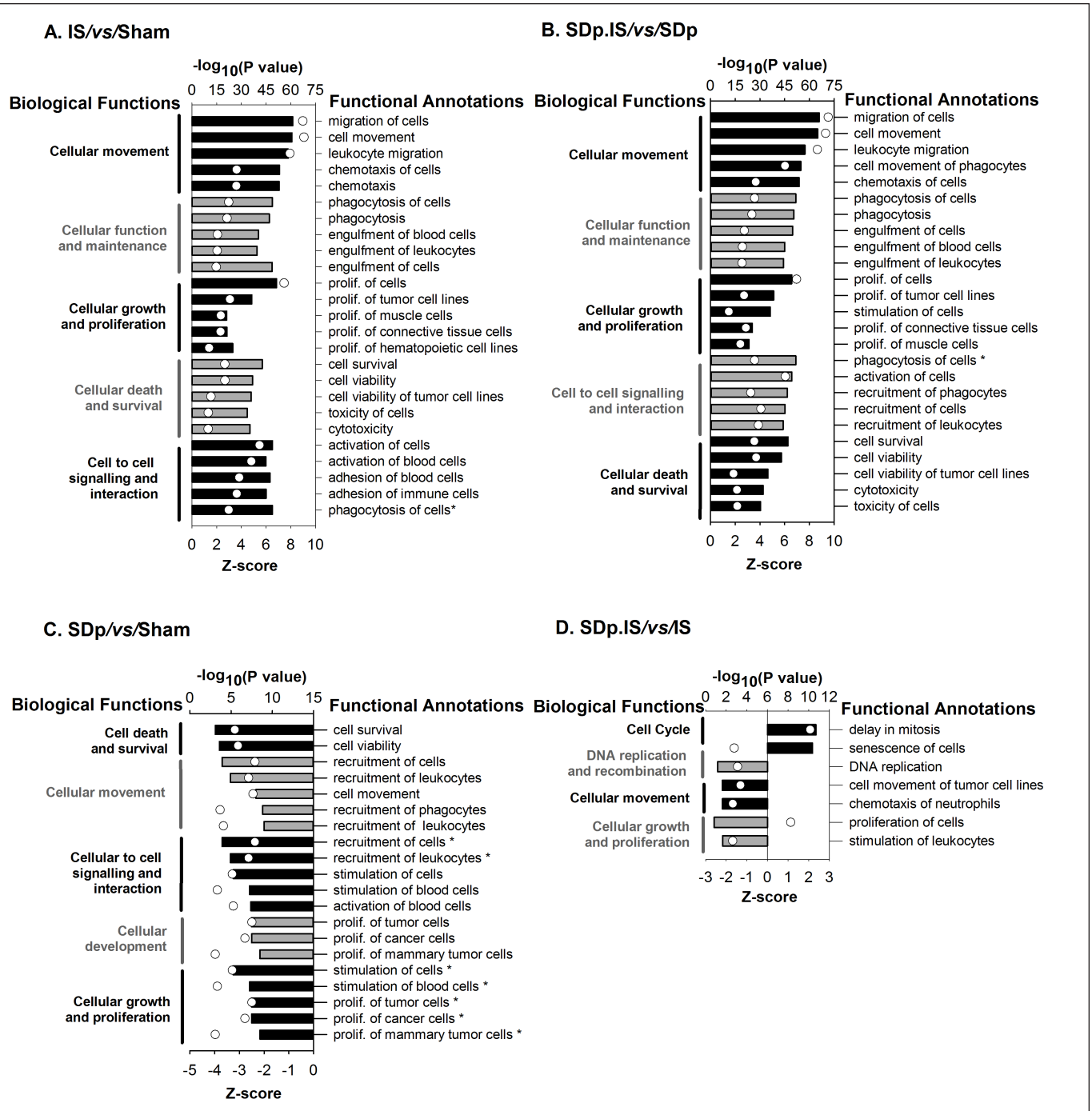

Figure 2—Biological functions (on the left of the graphs) and relative functional annotations (on the right) identified by Ingenuity Pathway Analysis (IPA) in the 4 different contrasts: **(A)** IS/vs/Sham; **(B)** SDp.IS/vs/SDp; **(C)** SDp/vs/Sham; **(D)** SDp.IS/vs/IS. Biological functions and functional annotations were identified based on two different metrics: z-score (bars - lower X axis) and P value (white dots - upper X axis). A z-score value ≥ 2 or ≤ 2 indicates that a function is predicted to be respectively increased or decreased within that contrast. The P value, calculated with the Fischer exact test, reflects the likelihood that the association between a set of genes in our dataset and a related biological function is significant. In this graph the top 5 biological functions and the relative top 5 functional annotations are summarized for each contrast, except for the SDp.IS/vs/IS in which only 4 functions were identified.

material). Among these 48 genes, the 2 most affected were *pMch* (0.915-fold; adj. P = 0.001) and *Hcrt* (2.209-fold; adj. P = 0.005).

Biological Functions and Canonical Pathways

Microarray dataset was analyzed by the downstream effects analysis in IPA (see Methods section). The 2 ischemia-associated contrasts (IS/vs/Sham and SDp.IS/vs/SDp; Figure 2A, 2B) showed the same top 5 biological functions. All the functional annotations relative to these functions were linked to the immune response and showed a positive activation z-score (≥ 2) (Figure 2A, 2B), indicating, as expected, a major activation of the immune system in ischemia. The same biological functions (except for *cellular function and maintenance)* were also identified in the SDp/vs/Sham contrast (Figure 2C). However, all functional annotations, again linked with immunity, showed a negative activation z-score (≤ 2), indicating that SDp in Sham

Table 1—Top five functional networks identified in the SDp.IS/*vs*/IS contrast with respective molecules involved.

ID	Genes in Network	P score	Focus Genes	Top Diseases and Functions
1	alcohol group acceptor phosphotransferase, APC (complex), APC-CDC20, APOC1, CCL13, CCNB1, CCNB2, CD300C, Cdc2, CDC20, Cdk, CDK1, CKS1B, Collagen Alpha1, Cr3, Cyclin A, Cyclin B, Cyclin E, ERK1/2, FBXO5, FOXM1, Histone H1, KIAA1524, LGALS1, Mek, NADPH oxidase, NEK2, OLR1, PLK1, PTTG1, Raf, RHOC, Sod, VLDL-cholesterol	36	18	• Cell Cycle; • Embryonic Development; • Cellular Movement.
2	ACPP, AGT, Alp, Angiotensin II receptor type 1, Ap1, ATF3, CASC5, CCL7, CENPI, Cg, CGA, Creb, ELF4, Fibrinogen, FSH, HCRT, Ifn gamma, IGFBP3, ITGA5, LDL, Lh, LY96, MAP2K1/2, MSR1, NFkB (complex), Nr1h, NUF2, PDGF BB, PLK4, PMCH, RIPK3, Tgf beta, TM4SF1, Tnf (family), Vegf	34	18	• Cell Morphology; • Embryonic Development; • Cell-To-Cell Signaling and Interaction.
3	CCNB2, CDKN3, CKS1B, CMTM7, DECR1, EBP, EMP3, ERBB2, ESPL1, FAM111A, GEMIN6, KIF22, KIF18A, KIF20A, KIF2C, LSM6, LSM7, MASTL, miR-16-5p (and other miRNAs w/seed AGCAGCA), PCSK6, PIEZO1, PLP2, PRIM1, RBM47, RGS22, SNRPA1, SNR, PF, SPAG5, SRPX, TBCB, Timd2, TIPIN, TM4SF1, UBC, UBE2S	34	17	• Cellular Assembly and Organization; • DNA Replication Recombination and Repair; • Cancer.
4	acetylcholine, APO-1, ARHGAP36, ARL11, ASB4, Bmyo, Ca2+, CALCR, CEACAM4, chloride, CXorf21, CXorf36, Eotaxin, FCN1, GLIPR1, Gm-Csf Receptor, Ifitm2, IgG4, IL13, ITIH3, MCHR2, miR-3194-5p (miRNAs w/seed GCCAGCC), miR-34a-5p (and other miRNAs w/seed GGCAGUG),miR-4667-3p (miRNAs w/seed CCCUCCU), PACE, PCSK1, PCSK7, PKC alpha/beta, PTH2R, SLAMF9, SLC17A6, SLC37A2, SPINT2, STAT3, TGFB1	28	15	• Cellular Function and Maintenance; • Molecular Transport; • Cell Cycle.
5	BCR (complex), CD14, CD86, CD180, Fc gamma receptor, Fcgr3, FCGR3A, HK3, Ifn, IFN alpha, IFN Beta, Ifnar, Ige, IgG, IgG1, IgG3, IgG2a, IgG2b, IgM, IkB, IL18, IL12 (complex), IL12 (family), IL1R1, Immunoglobulin, ITGAX, MHC Class II (complex), PBK, PIK3AP1, PLAC8, PLC, PKB gamma, SPI1, Tlr, VAV	26	12	• Inflammatory response; • Hematological System Development and Function

Functional networks were identified using Ingenuity Pathway Analysis (IPA) software. The P scores used to rank networks on the IPA are derived from P values. The P value is the probability of finding a certain number of focus genes in the set of the total number of genes randomly selected from the Global Molecular Network. It is calculated using Fisher exact test. Since interesting P values are typically quite low, the P score is defined as: P score = −log10 (P value).

ACPP, acid phosphatase prostate; ALP, alkaline phosphatase; Ap1, adaptor-related protein complex 1; APC, adenomatous polyposis coli; APO-1, apoptosis antigen 1; APOC1, apolipoprotein C-1; ARHGAP36, rho GTPase activating protein 36; ARL11, ADP-ribosylation factor-like 11; ASB4, ankyrin repeat and SOCS box containing 4; ATF3, activating transcription factor 3; BCR, breakpoint cluster region; Bmyo, beta-myosin heavy chain; CALCR, calcitonin receptor; CASC5, cancer susceptibility candidate 5; CCL13, chemokine (C-C motif) ligand 13; CCNB1, cyclin B1; CCNB2, cyclin B2; CDC2, cell division cycle 2; CDC20, cell division cycle 20; CDK1, cyclin-dependent kinase 1 ; CDKN3, cyclin-dependent dinase inhibitor 3; CEACAM4, carcinoembryonic antigen-related cell adhesion molecule 4; CENPI, centromere protein I; CKS1B, protein kinase regulatory subunit 1B; CDC28, cell division cycle 28; CMTM7, CKLF-like MARVEL transmembrane domain containing 7; Cr3, complement receptor 3 ; Creb, cAMP (cyclic adenosine monophosphate) responsive element binding protein; CXorf21, chromosome X open reading frame 21; CXorf36, chromosome X open reading frame 36; DECR1, 2,4-dienoyl CoA reductase 1, mitochondrial; EBP, emopamil binding protein; ELF4, E74-like factor 4 ; EMP3, epithelial membrane protein 3; ERBB2, Erb-B2 receptor tyrosine kinase 2; ERK1/2, extracellular signal-regulated kinases 1/2; ESPL1, extra spindle pole bodies homolog 1; FAM111A, family with sequence similarity 111 member A; FBXO5, F-box protein 5; FCGR3A, cluster of differentiation 16; FCN1, ficolin (collagen/fibrinogen domain containing) 1; FOXM1, forkhead box M1; GLIPR1, GLI (gliobastoma) pathogenesis-related 1; Gm-Csf, granulocyte-macrophage - colony stimulating factor; HK3, hexokinase 3; Ifitm2, interferon induced transmembrane protein 2; IFN, interferon; Ifnar, interferon (alpha, beta and omega) receptor 1; IgG, immunoglubulin E; IGFBP3, insulin-like growth factor binding protein 3; IgG, immunoglubulin G; IgM, immunoglubulin M; IkB, kappa light polypeptide gene enhancer in B-cells inhibitor; IL12, interleukin 12; IL13, interleukin 13; IL18, interleukin 18; ITGA5, integrin alpha 5 ; ITIH3, inter-alpha-trypsin inhibitor heavy chain 3; KIF18A, kinesin family member 18A; KIF20A, kinesin family member 20A; KIF22, kinesin family member 22; KIF2C, kinesin family member 2C; LDL, low density lipoprotein; LGALS1, lectin galactoside-binding soluble 1; LSM6, like Sm 6; LSM7, like Sm 6; LY96, lymphocyte antigen 96; MAP2K1/2, mitogen-activated protein kinase 1/2; MASTL, microtubule associated serine/threonine kinase-like; MCHR2, melanin concentrating hormone receptor 2; MEK, mitogen-activated protein kinase; MHC, major histocompatibility complex,; NADPH, nicotinamide adenine dinucleotide phosphate ; NEK2, NIMA-related kinase 2; OLR1, oxidized low density lipoprotein (lectin-like) receptor 1; PACE, paired basic amino acid cleaving enzyme; PBK, PDZ binding kinase; PCSK1, proprotein convertase subtilisin/kexin type 1; PCSK6, proprotein convertase subtilisin/kexin type 6; PCSK7, proprotein convertase subtilisin/kexin type 7; PF, platelet factor; PIEZO1, piezo-type mechanosensitive ion channel component 1; PIK3AP1, phosphoinositide-3-kinase adaptor protein 1; PKB, protein kinase B; PKC, protein kinase C; PLAC8, placenta-specific 8; PLC, phospholipase C ; PLP2, proteolipid protein 2; PRIM1, primase DNA polypeptide; PTH2R, parathyroid hormone 2 receptor; Raf, rapidly accelerated fibrosarcoma ; RBM47, RNA binding motif protein 47; RGS22, regulator of G-protein signaling 22; RHOC, Ras homolog family member C; SLAMF9, signaling lymphocytic activation molecule family member 9; SLC17A6, solute carrier family 17 (vesicular glutamate transporter) member 6; SLC37A2, solute carrier family 37 (glucose-6-phosphate transporter) member 2; SNR, small nuclear ribonucleoprotein; SNRPA1, small nuclear ribonucleoprotein polypeptide A1; SOD, superoxide dismutase; SPAG5, sperm associated antigen 5; SPI1, Spi-1 proto-oncogene; SPINT2, serine peptidase inhibitor Kunitz type 2; SRPX, sushi-repeat containing protein, X-linked; STAT3, signal transducer and activator of transcription 3; TBCB, tubulin folding cofactor B; TGFB1, transforming growth factor beta 1; Timd2, T cell immunoglobulin and mucin domain containing ; TIPIN, TIMELESS interacting protein; Tlr, toll like receptor; TM4SF1, transmembrane 4 L six family member 1; UBC, ubiquitin C; UBE2S2K, ubiquitin-conjugating enzyme E2S; VLDL, very low density lipoprotein.

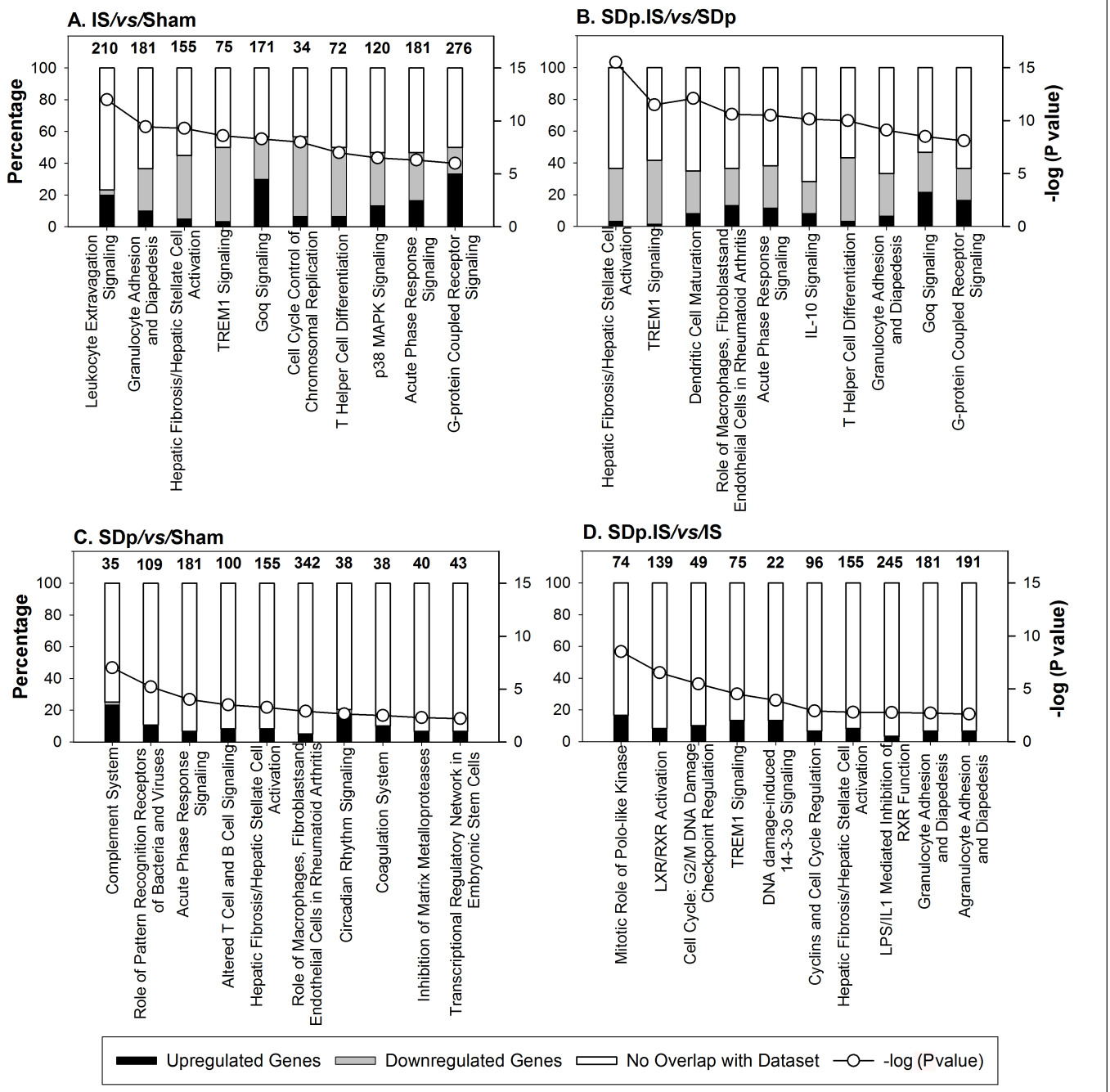

Figure 3—Canonical pathways identified by Ingenuity Pathway Analysis (IPA) in the 4 different contrasts: **(A)** IS/vs/Sham; **(B)** SDp.IS/vs/SDp; **(C)** SDp/vs/Sham; **(D)** SDp.IS/vs/IS. The number of focus genes in each pathway are shown as percentages of all the genes associated with that pathways (numbers on top of bars). Expression changes are shown as upregulated (black bars) or downregulated (gray bars). The P value associated with a pathway is a measure of the likelihood that the association between the set of focus genes and the given pathway is due to random chance. P values less than 0.05 indicate a statistically significant, non-random association. The P value is calculated using the right-tailed Fisher exact test. Respective P values are indicated as white dots (right Y axis) on each graph.

animals induced an inhibition of the immune system. *Cellular growth and proliferation* was also identified in the SDp.IS/vs/IS contrast, with a negative z-score for the functional annotations confirming an inhibiting effect of SDp on the immune function (Figure 2D). In the SDp.IS/vs/IS contrast we found 3 biological functions that were exclusive to this condition: *cell cycle, DNA replication and repair* and *cellular assembly and organization*. For this contrast *delay in mitosis* and *senescence of cells* were the only 2 functional annotations with a positive z-score, while all the others showed a negative z-score (Figure 2D). The direction of the activation of the functional annotations in the SDp.IS/vs/IS contrast indicates that SDp preconditioning induced a further delay in mitosis and inhibits DNA replication.

The inhibiting effect of SDp on the immune system and on the cell cycle regulation of ischemic rats was confirmed by

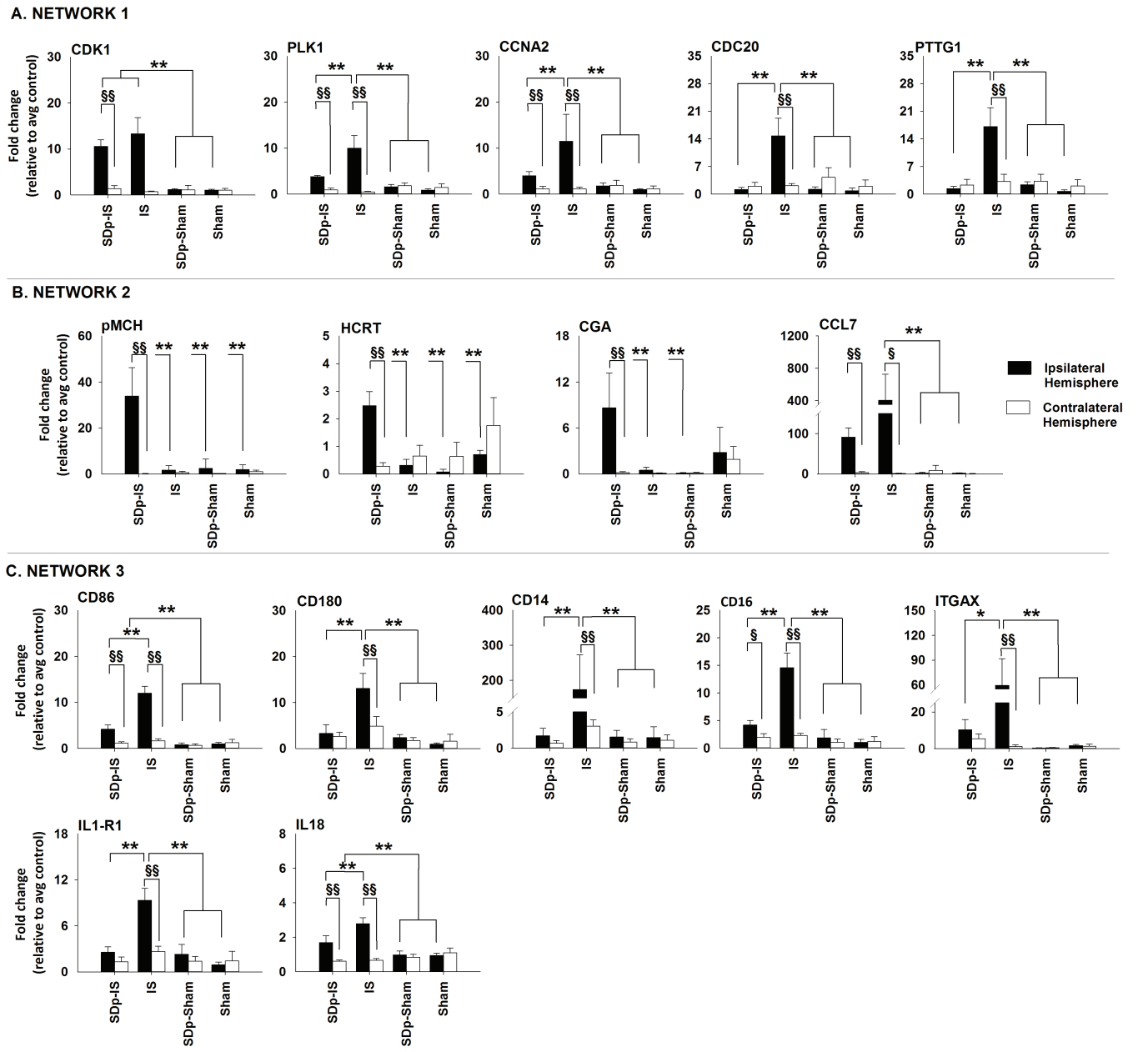

Figure 4—Expression of selected genes at 3 days after stroke in ipsilateral (dark bar) and contralateral hemisphere (white bar) within the 3 functional networks selected. Gene expression (mean ± standard deviation) was assessed by qRT-PCR in rats belonging to the 4 experimental groups: i. SDp.IS; ii. IS; iii. SDp.Sham, and iv. Sham. The candidate genes were selected based on fold change (≤ 1.5 or ≥ 1.5) and adj. P values observed in the microarray dataset. GAPDH was used as the reference gene. The ΔΔCt method was used to determine the fold change in gene expression. Statistics were performed by mean of a 2-way ANOVA (factors: group and hemisphere) and post hoc analysis with Tukey correction were run afterwards. Asterisks (*) indicate a statistical difference between groups (*P ≤ 0.05; **P ≤ 0.01) whereas double-S (§) indicate a statistical difference between ipsilateral and contralateral hemisphere in the same group (§ P ≤ 0.05; §§ P ≤ 0.01).

canonical pathways (Figure 3). Six canonical pathways, all associated with inflammatory response and all showing an up-regulation of the genes involved, were common between the ischemia associated contrast (Figure 3A, 3B). Two of these pathways were also found in the SDp.IS/vs/IS (Figure 3D); however, for this contrast genes were mostly downregulated. The only pathway common among all conditions (*hepatic fibrosis/hepatic stellate cell activation*) showed also this trend, with several genes upregulated in contrasts associated with the IS effect (Figure 3A, 3B) and downregulated in SDp.IS/vs/IS (Figure 3D) and SDp/vs/Sham (Figure 3C). The canonical pathways specific to SDp.IS/vs/IS (Figure 3D) were associated with inflammation (*LXR/RXR activation and LPS/IL-1 mediated inhibition of RXR function*) and cell cycle regulation (*mitotic roles of Polo-Like Kinase*, *Cell cycle: G2/M checkpoint regulation*, *DNA damage induced 14-3-3σ signalling* and *Cyclins*), and they all showed a general downregulation of the genes involved.

Table 2—Expression of selected genes 3 and 7 days after ischemia in IS and SDp.IS.

	IS		SDp.IS	
	Day 3	Day 7	Day 3	Day 7
Cell Cycle				
CDK1	13.35 ± 3.50	5.55 ± 1.97°°	10.60 ± 1.39	3.93 ± 1.02°°
PLK1	10.00 ± 2.71	1.86 ± 0.77°°	3.81 ± 0.21*	1.05 ± 0.43°°
CCNA2	11.46 ± 5.85	5.87 ± 3.46	4.01 ± 0.90**	4.56 ± 2.08
CDC20	17.13 ± 4.77	9.31 ± 3.82	1.18 ± 0.51**	7.42 ± 2.48°°
PTTG1	14.80 ± 4.42	13.17 ± 3.21	1.39 ± 0.57**	9.54 ± 3.55°
Inflammation				
CD86	12.00 ± 1.47	22.51 ± 11.69	4.17 ± 0.93**	16.65 ± 6.60°
CD180	13.07 ± 3.27	31.87 ± 15.41	3.30 ± 1.89**	28.30 ± 8.24°°
CD14	174.18 ± 98.46	203.63 ± 93.03	1.69 ± 1.05**	156.87 ± 51.63°°
FCGR3A	14.58 ± 2.64	26.52 ± 14.22	4.17 ± 0.81**	10.43 ± 3.74°
IL1-R1	9.33 ± 1.54	8.48 ± 1.82	2.56 ± 0.70**	4.57 ± 1.26*
ITGAX	59.36 ± 32.21	184.43 ± 70.87°	10.29 ± 5.57*	88.67 ± 29.50*,°
IL18	2.78 ± 0.36	4.10 ± 1.91	1.69 ± 0.40**	3.51 ± 1.61
Neuroendocrine				
pMCH	1.74 ± 1.87	0.09 ± 0.04	33.91 ± 12.33**	0.09 ± 0.03°°
HCRT	0.32 ± 0.21	0.43 ± 0.34	2.48 ± 0.51**	0.24 ± 0.20°°
CGA	0.50 ± 0.41	0.35 ± 0.40	8.62 ± 4.57*	0.32 ± 0.29°

Values are expressed as the fold change from the average control values ± standard deviation. Statistical differences between experimental groups at the same time point are indicated by asterisks (t-test; *P < 0.05, **P < 0.01), whereas dots indicate statistical differences between time points in the same experimental group (t-test; °P < 0.05, °°P < 0.01). SDp.IS, sleep deprivation followed by ischemia; IS, ischemia; CCNA2, cyclin A2; CD14, cluster of differentiation 14; CD180, cluster of differentiation 180; CD86, cluster of differentiation 86; CDC20, cell-division cycle protein 20; CDK1, cyclin-dependent kinase 1; CGA, glycoprotein hormones-alpha polypeptide; FCGR3A, cluster of differentiation 16; HCRT, hypocretin; IL18, interleukin 18; IL1-R1, interleukin-1 receptor 1; ITGAX, integrin, alpha X; PLK1, polo-like kinase 1; pMCH, melanin concentrating hormone; PTTG1, pituitary tumor-transforming 1; TSH, thyroid stimulating hormone.

Validation of Microarray Results with qRT-PCR

The 18 genes investigated with qRT-PCR were selected within the top 5 functional networks identified by IPA for the SDp.IS/vs/IS contrast (Table 1). Among these 5 networks, on the basis of the analysis of biological functions and canonical pathways only 3 (network 1, 2, and 4) were selected for further investigations (Figure 4). Selected genes included the 5 genes that were the most upregulated (*pMch, Cga, Hcrt, Calcr*, and *Agt*) and downregulated (*Itgax, Ccl7, Cd14, Ccna2*, and *Cdk1*). Moreover, based on the fold change and P values from the affimetrix dataset, we chose to asses 3 more genes within the first network and 5 more genes within the fourth network.

Figure 4A shows the expression 3 days after stroke of the genes investigated within the first network. All genes were significantly increased in the ipsilateral hemisphere of the IS group when compared both to the contralateral hemisphere in the same group and to the ipsilateral hemisphere in all others groups investigated. In SDp.IS group no genes except *Cdk1* were significantly different in the ipsilateral hemisphere when compared to the same hemisphere of the 2 control groups Sham and SDp. However, when compared to the contralateral hemisphere within the same group, a significant increase in the expression of *Cdk1*, *Plk1*, and *Ccna2* was observed. In contrasts, the expression of the genes *Cdc20* and *Pttg1* was not different between the 2 hemispheres. After 7 days from stroke no differences were detected between groups for any of the aforementioned genes (Table 2).

Within the second network 5 genes were investigated (Figure 4B). *pMch*, *Hcrt*, and *Cga* were significantly increased in the ipsilateral hemisphere of SDp.IS animals when compared to the contralateral hemisphere. This increase was also significant when compared to all the other experimental groups, with the exception of *Cga*, which was not different from the Sham group. For *AGT*, no difference in the expression was observed between hemispheres or between groups (data not shown). *Ccl7* showed a significant increase of gene expression in the ipsilateral hemisphere of both IS and SDp.IS groups compared to the contralateral hemisphere. However no difference was observed between SDp.IS animals and the other experimental groups; for this reason, no further analysis were performed on this gene. At day 7, due to a significant decrease with respect to day 3, the expression level of *pMch*, *Hcrt* and *Cga* was no longer different between the SDp.IS and the IS group (Table 2).

Similar to what observed in network 1, in network 4 (Figure 4C) the genes in IS group were significantly increased in the ipsilateral hemisphere compared both to the contralateral hemisphere and to all the other groups. In the SDp.IS group a significant increase in the ipsilateral hemisphere was observed only for *Cd86, Cd16*, and *IL18*; however, this increase was lower than that observed in IS. No statistical difference was observed between SDp.IS and the control groups (Sham and SDp groups) with the exception of *Cd86* and *IL1-r1*. Gene expression at day 7 was similar between SDp.IS and IS, except for *IL1-r1* and *Itgax,* due to a significant increase in the gene

levels observed in SDp.IS group with respect to day 3 (Table 2). No differences were observed in the IS group between the 2 time points (Table 2).

Peripheral Sex Hormone Levels

To assess if the alterations in gene expression of *pMch*, *Hcrt*, and *Cga* had an effect on the regulation of sex hormones at a peripheral level, we measured 17β-estradiol and testosterone in the serum of rats from SDp.IS and IS groups both at 3 and 7 days after stroke (Figure 5). Both hormones were differently regulated in SDp.IS compared to IS group at 3 days after stroke. In particular, the plasma concentration of 17β-estradiol was higher in the SDp.IS, whereas testosterone level was lower. However no difference in 17β-estradiol and testosterone level was observed between Sham group and both IS and SDp.IS animals (data not shown). After 7 days from stroke a decrease of 17β-estradiol with respect to day 3 was observed in both groups, and no more difference was observed between groups. Instead, testosterone levels increased from day 3 to day 7 in SDp.IS, reaching similar levels to those observed in the IS group at both 3 and 7 days.

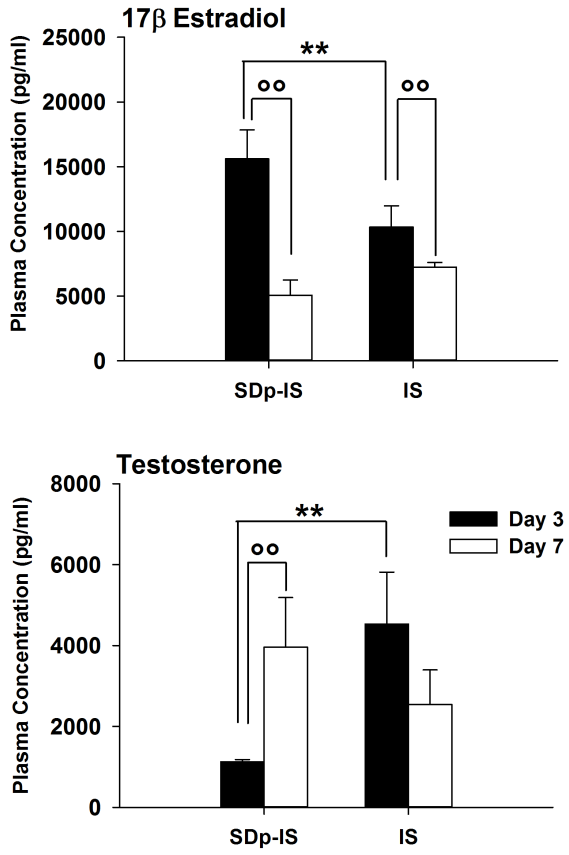

Figure 5—Concentration of 17β estradiol and testosterone in the plasma of rats of the SDp.IS and IS group at 3 (black bars) and 7 days after stroke (white bars) assessed by ELISA immunoassay. Data are presented as mean ± standard deviation. Statistics were performed by mean of a 2-way ANOVA (factors: group and day) and post hoc analysis with Tukey correction were run afterwards. Asterisks (*) indicate a statistical difference between groups (**P ≤ 0.01), whereas dots (°) indicate a statistical difference between days within the same group (°°P ≤ 0.01).

DISCUSSION

Several studies have reported that SDp before ischemia induces neuroprotection,[8,9] leading to a significant reduction of infarct volume after 7 days from stroke.[10,11] This study confirms this effect and provides for the first time a comprehensive investigation of the molecular pathways involved. We identified three main functions which are altered by performing SDp prior to ischemia: inflammatory response, cell cycle, and neuroendocrine regulation. Although microarray analysis was performed 4 days prior to when evidence of ischemic tolerance was observed, the process essential for the improvement of the outcome are likely to be already activated at this time point. Since all the functions we found altered at day 3 returned to baseline levels by day 7, when the reduction in the lesion was observed in the preconditioned animals, it is possible to assume that the critical time window for the action of the neuroprotective mechanisms induced by pre-ischemic SDp is within 7 days from stroke.

In general, the molecular response to ischemic damage was characterized, as expected,[28] by an upregulation of a large number of genes involved in immune response and cell cycle regulation. However, both the inflammatory response and the cell division mechanisms were reduced after SDp preconditioning. A reduction of the inflammatory response to ischemia has also been reported for other preconditioning treatments.[12] It has been suggested that the neuroprotective effect of these stimuli is exerted by a pre-activation of the immune system before stroke. Several forms of preconditioning produce an inflammatory response through the activation of toll like receptors (TLRs) leading to the subsequent activation of transcription factor nuclear factor κB (NFκB).[13] The importance of the TLRs activation in mediating ischemic tolerance has also been confirmed by direct administration of TLR ligands.[29] In addition, sleep loss has been reported to induce alterations in immune parameters,[30–33] and interestingly, the molecular mechanisms underlying these modifications have been linked to the NFκB pathway.[32] The fact that the two inflammatory pathways specifically altered in SDp.IS/vs/IS contrast are mediated by TLRs activity is therefore noteworthy. LXR and RXR are two types of nuclear receptors which regulate inflammation and lipid metabolism and that are activated through TLRs.[34] Moreover, several genes linked to TLR4 activity (*Cd14*, *Cd180*, and *Il1-r*) are not only downregulated in SDp.IS animals with respect to the IS group, but their expression is not different with respect to the control groups. Together these results suggests that the neuroprotective effect of SDp could be partially driven by a post-ischemic attenuation of the TLRs response.

For cell cycle regulation, biological functions and canonical pathway analysis indicated an increased delay in mitosis and an inhibition of DNA replication in SDp.IS rats. Moreover also several genes identified in the first network (*Cdk1, Plk1, Ccna2, Cdc20*, and *Pttg*) were implicated once again in the entry of cells into mitosis and in other processes such the G1/S transition, differentiation, proliferation, and cell death. Cell cycle checkpoints are activated to ensure correct completion of critical events such as DNA replication and chromosome segregation. Activation of checkpoints in response to DNA damage

and inhibition of DNA replication are known to lead to a reversible cell cycle arrest to allow time for damage repair.[35] It has actually been demonstrated that the inhibition of the cell cycle, either by administration of inhibitors or modulation of cell cycle related genes, suppresses neuronal death or provides neuroprotection after ischemia.[36–38] This observation is consistent with the fact that rats treated with pre-stroke SDp display a reduction in apoptosis.[10] An inhibition of cell cycle mechanisms with beneficial effects on stroke has been reported for mild ischemia and hypoxia preconditioning[39,40]; however, this is the first time that such effect has been linked with SDp. This effect was compared with adaptive neuroprotective strategies seen during hibernation as the activation of some endogenous genetic mechanisms inducing tolerance to low oxygen levels.[39,40] Rats sleep deprived for 6 h prior to stroke showed a significant sleep rebound characterized by an increase of 30% of total sleep time in the first 12 h of the acute phase of stroke recovery.[11] The general decrease in the energetic demand of both the brain and the body[17,19,41] and the concomitant lower temperature[42,43] characterizing sleep might therefore induce neuroprotective mechanisms similar to those observed in hibernating animals.

The last pathway identified in this study was the only one including genes which were upregulated by SDp preconditioning. In particular three of these genes, *PMch, Hcrt and Cga,* were the most upregulated of the entire dataset. *PMch* and *Hcrt* were expressed exclusively in the SDp.IS/vs/IS contrast, whereas *Cga* was common in the two contrasts associated with IS. However *Cga* showed an inverse regulation in the two conditions, being downregulated by ischemia alone and upregulated with SDp preconditioning. This was particularly surprising as 80% of the genes shared between SDp.IS/vs/IS and IS/vs/Sham showed instead the opposite trend. It has been shown already that *Hcrt* alters the pathological mechanisms involved in brain ischemia and has a neuroprotective effect.[44,45] Instead, to our knowledge, this is the first time that *pMch* has been identified as a possible neuroprotective peptide. Mch and Hcrt neurons both represent key components of the system that regulates the sleep-wake cycle.[46,47] Both peptides are involved also in other functions such as feeding behavior and energy balance and homeostasis.[48–52] As far as the sleep-wake cycle is concerned Hcrt neurons play an important role in arousal regulation,[53,54] whereas Mch neurons are more involved in the regulation of sleep states, particularly REM sleep. Prolonged activation of Mch neurons both pharmacologically[55] and by repeated optogenetic stimulation[56] induces both NREM and REM sleep. Mch neurons are strongly activated during homeostatic sleep rebound, discharging maximally during REM sleep.[57,58] REM sleep is usually significantly reduced after ischemia[4,59]; however, animals sleep deprived before stroke show a sleep rebound characterized by an increase in REM sleep amount.[11] The increase in *pMch* observed in our animals might be therefore linked to the REM sleep rebound observed in the acute phase of stroke. The mechanisms through which Mch can induce neuroprotection are although unclear and further studies are necessary. However Mch together with Hcrt and Cga are involved in the control of endocrine functions, known to be neuroprotective. Mch and Hcrt, when injected in the hypothalamus, can indeed exert stimulatory effects on the gonadotropin-releasing hormone,[60–62] which is in turn responsible for the release of luteinizing hormone (LH) and follicle stimulating hormone (FSH). Moreover Cga constitutes the common alpha subunit of four glycoprotein hormones: LH, FSH, chorionic gonadotropin (CG), and thyroid stimulating hormone (TSH).[63] Our results showed a peripheral increase of 17β-estradiol level 3 days after stroke and a concomitant decrease in testosterone. It is well accepted that estradiol provides robust neuroprotection in a variety of acute experimental brain injury models including stroke,[64,65] whereas the role of testosterone is still not completely clarified. However brain damaging effects of testosterone treatment have been reported in a rodent model of stroke[66] and, in vitro.[67] Nevertheless reactive gliosis after neuronal injury seemed to be downregulated by testosterone but this effect has been largely attributed to testosterone conversion into estradiol.[68] We therefore suggest that SDp preconditioning may affect the hypothalamic-pituitary-adrenal axis inducing modifications in the peripheral levels of sex-hormones which could ultimately play a role in neuroprotection.

CONCLUSIONS

The microarray analysis carried out in this study is the first to investigate the changes in gene expression elicited by SDp preconditioning. Besides confirming two mechanisms that appear to be common to several forms of preconditioning treatments (i.e., downregulation of the inflammatory responses and inhibition of the cell cycle) we discovered a novel pathway that concerned endocrine signaling and that included genes such *pMch*, *Hcrt*, and *Cga* that has not been previously implicated in SDp preconditioning or other preconditioning treatments. Our study provides the basis for exploring new approaches for the development of potential therapeutic and neuroprotective intervention for clinical use in stroke patients. In order to better understand the role and the mechanisms of this pathway in mediating neuroprotection, investigation of the expression of *pMch* and *Hcrt* and their relationship with sleep behavior and metabolism during both the acute and sub-acute phase of stroke, are currently undergoing in our laboratory.

ABBREVIATIONS

AGT, angiotensin
Ccl7, chemokine (C-C motif) ligand 7
Ccna2, cyclin A2
Cd14, cluster of differentiation 14
Cd16/Fcgr3a, cluster of differentiation 16
Cd180, cluster of differentiation 180
Cd86, cluster of differentiation 86
Cdc20, cell-division cycle protein 20
Cdk1, cyclin-dependent kinase 1
CG, chorionic gonadotropin
Cga, glycoprotein hormones-alpha polypeptide
FSH, follicle stimulating hormone
GAPDH, glyceraldehyde-3-phosphate dehydrogenase
Hcrt, hypocretin
IL18, interleukin 18
IL1-r1, interleukin-1 receptor 1
IS, ischemia
Itgax, integrin, alpha X

LH, luteinizing hormone
Plk1, polo-like kinase 1
pMch, melanin concentrating hormone
Pttg1, pituitary tumor-transforming 1
SDp, sleep deprivation
TSH, thyroid stimulating hormone

ACKNOWLEDGMENTS

Microarray analysis were performed at the Genomic Technologies Facility (GTF) of the University of Lausanne. The authors would like to thank Leonore Wigger at GTF for the technical work and Prof. Paul Franken from the Center for Integrative Genomics of the University of Lausanne for the initial guidance and advice and comments of the manuscript. Remarks and suggestions from Prof. Antoine Adamantidis, director of the Zentrum für Experimentelle Neurologie at the Inselspital in Bern, were also appreciated. Moreover, the support with Ingenutity Pathway Analysis software from Cedric Simillion at the Interfaculty Bioinformatics Unit of the University of Bern is gratefully acknowledged.

DISCLOSURE STATEMENT

This was not an industry supported study. The authors have indicated no financial conflicts of interest. Microarray data were uploaded on *ArrayExpress* database (E-MTAB-3148).

REFERENCES

1. Fonarow GC, Smith EE, Saver JL, et al. Timeliness of tissue-type plasminogen activator therapy in acute ischemic stroke: patient characteristics, hospital factors, and outcomes associated with door-to-needle times within 60 minutes. Circulation 2011;123:750–8.
2. Grandner MA, Jackson NJ, Pak VM, Gehrman PR. Sleep disturbance is associated with cardiovascular and metabolic disorders. J Sleep Res 2012;21:427–33.
3. Hermann DM, Bassetti CL. Sleep-related breathing and sleep-wake disturbances in ischemic stroke. Neurology 2009;73:1313–22.
4. Gao B, Cam E, Jaeger H, Zunzunegui C, Sarnthein J, Bassetti CL. Sleep disruption aggravates focal cerebral ischemia in the rat. Sleep 2010;33:879–87.
5. Zunzunegui C, Gao B, Cam E, Hodor A, Bassetti CL. Sleep disturbance impairs stroke recovery in the rat. Sleep 2011;34:1261–9.
6. Gao B, Kilic E, Baumann CR, Hermann DM, Bassetti CL. Gamma-hydroxybutyrate accelerates functional recovery after focal cerebral ischemia. Cerebrovasc Dis 2008;26:413–9.
7. Hodor A, Palchykova S, Baracchi F, Noain D, Bassetti C. Baclofen facilitates sleep, neuroplasticity and recovery after stroke in rats. Ann Clin Transl Neurol 2014;1:765–77.
8. Hsu JC, Lee YS, Chang CN, Ling EA, Lan CT. Sleep deprivation prior to transient global cerebral ischemia attenuates glial reaction in the rat hippocampal formation. Brain Res 2003;984:170–81.
9. Weil ZM, Norman GJ, Karelina K, et al. Sleep deprivation attenuates inflammatory responses and ischemic cell death. Exp Neurol 2009;218:129–36.
10. Moldovan M, Constantinescu AO, Balseanu A, Oprescu N, Zagrean L, Popa-Wagner A. Sleep deprivation attenuates experimental stroke severity in rats. Exp Neurol 2010;222:135–43.
11. Cam E, Gao B, Imbach L, Hodor A, Bassetti CL. Sleep deprivation before stroke is neuroprotective: a pre-ischemic conditioning related to sleep rebound. Exp Neurol 2013.
12. Dirnagl U, Becker K, Meisel A. Preconditioning and tolerance against cerebral ischaemia: from experimental strategies to clinical use. Lancet Neurol 2009;8:398–412.
13. Kariko K, Weissman D, Welsh FA. Inhibition of toll-like receptor and cytokine signaling--a unifying theme in ischemic tolerance. J Cereb Blood Flow Metab 2004;24:1288–304.
14. Cirelli C, Gutierrez CM, Tononi G. Extensive and divergent effects of sleep and wakefulness on brain gene expression. Neuron 2004;41:35–43.
15. Mackiewicz M, Naidoo N, Zimmerman JE, Pack AI. Molecular mechanisms of sleep and wakefulness. Ann N Y Acad Sci 2008;1129:335–49.
16. Durukan A, Tatlisumak T. Acute ischemic stroke: overview of major experimental rodent models, pathophysiology, and therapy of focal cerebral ischemia. Pharmacol Biochem Behav 2007;87:179–97.
17. Kennedy C, Gillin JC, Mendelson W, et al. Local cerebral glucose utilization in non-rapid eye movement sleep. Nature 1982;297:325–7.
18. Kong J, Shepel PN, Holden CP, Mackiewicz M, Pack AI, Geiger JD. Brain glycogen decreases with increased periods of wakefulness: implications for homeostatic drive to sleep. J Neurosci 2002;22:5581–7.
19. Netchiporouk L, Shram N, Salvert D, Cespuglio R. Brain extracellular glucose assessed by voltammetry throughout the rat sleep-wake cycle. Eur J Neurosci 2001;13:1429–34.
20. Franken P, Dijk DJ, Tobler I, Borbely AA. Sleep deprivation in rats: effects on EEG power spectra, vigilance states, and cortical temperature. Am J Physiol 1991;261:R198–208.
21. Lack LC, Gradisar M, Van Someren EJ, Wright HR, Lushington K. The relationship between insomnia and body temperatures. Sleep Med Rev 2008;12:307–17.
22. Ramanathan L, Gulyani S, Nienhuis R, Siegel JM. Sleep deprivation decreases superoxide dismutase activity in rat hippocampus and brainstem. Neuroreport 2002;13:1387–90.
23. Singh R, Kiloung J, Singh S, Sharma D. Effect of paradoxical sleep deprivation on oxidative stress parameters in brain regions of adult and old rats. Biogerontology 2008;9:153–62.
24. Chen ST, Hsu CY, Hogan EL, Maricq H, Balentine JD. A model of focal ischemic stroke in the rat: reproducible extensive cortical infarction. Stroke 1986;17:738–43.
25. Ashwell KW, Paxinos G, Watson CR. Precerebellar and vestibular nuclei of the short-beaked echidna (Tachyglossus aculeatus). Brain Struct Funct 2007;212:209–21.
26. Junge CE, Sugawara T, Mannaioni G, et al. The contribution of protease-activated receptor 1 to neuronal damage caused by transient focal cerebral ischemia. Proc Natl Acad Sci U S A 2003;100:13019–24.
27. Chomczynski P, Mackey K. Short technical reports. Modification of the TRI reagent procedure for isolation of RNA from polysaccharide- and proteoglycan-rich sources. BioTechniques 1995;19:942–5.
28. Gidday JM. Cerebral preconditioning and ischaemic tolerance. Nat Rev Neurosci 2006;7:437–48.
29. Marsh BJ, Williams-Karnesky RL, Stenzel-Poore MP. Toll-like receptor signaling in endogenous neuroprotection and stroke. Neuroscience 2009;158:1007–20.
30. Irwin MR, Carrillo C, Olmstead R. Sleep loss activates cellular markers of inflammation: sex differences. Brain Behav Immun 2010;24:54–7.
31. Matsumoto Y, Mishima K, Satoh K, et al. Total sleep deprivation induces an acute and transient increase in NK cell activity in healthy young volunteers. Sleep 2001;24:804–9.
32. Opp MR. Sleep and psychoneuroimmunology. Neurol Clin 2006;24:493–506.
33. Vgontzas AN, Zoumakis E, Bixler EO, et al. Adverse effects of modest sleep restriction on sleepiness, performance, and inflammatory cytokines. J Clin Endocrinol Metab 2004;89:2119–26.
34. Freeman MW, Moore KJ. eLiXiRs for restraining inflammation. Nat Med 2003;9:168–9.
35. Singh SV, Herman-Antosiewicz A, Singh AV, et al. Sulforaphane-induced G2/M phase cell cycle arrest involves checkpoint kinase 2-mediated phosphorylation of cell division cycle 25C. J Biol Chem 2004;279:25813–22.
36. Wang W, Redecker C, Yu ZY, et al. Rat focal cerebral ischemia induced astrocyte proliferation and delayed neuronal death are attenuated by cyclin-dependent kinase inhibition. J Clin Neurosci 2008;15:278–85.
37. Zhu Z, Zhang Q, Yu Z, et al. Inhibiting cell cycle progression reduces reactive astrogliosis initiated by scratch injury in vitro and by cerebral ischemia in vivo. Glia 2007;55:546–58.
38. Osuga H, Osuga S, Wang F, et al. Cyclin-dependent kinases as a therapeutic target for stroke. Proc Natl Acad Sci U S A 2000;97:10254–9.
39. Prasad SS, Russell M, Nowakowska M, Williams A, Yauk C. Gene expression analysis to identify molecular correlates of pre- and post-conditioning derived neuroprotection. J Mol Neurosci 2012;47:322–39.

40. Stenzel-Poore MP, Stevens SL, Xiong Z, et al. Effect of ischaemic preconditioning on genomic response to cerebral ischaemia: similarity to neuroprotective strategies in hibernation and hypoxia-tolerant states. Lancet 2003;362:1028–37.
41. Dash MB, Tononi G, Cirelli C. Extracellular levels of lactate, but not oxygen, reflect sleep homeostasis in the rat cerebral cortex. Sleep 2012;35:909–19.
42. Busto R, Dietrich WD, Globus MY, Ginsberg MD. Postischemic moderate hypothermia inhibits CA1 hippocampal ischemic neuronal injury. Neurosci Lett 1989;101:299–304.
43. Busto R, Dietrich WD, Globus MY, Ginsberg MD. The importance of brain temperature in cerebral ischemic injury. Stroke 1989;20:1113–4.
44. Kitamura E, Hamada J, Kanazawa N, et al. The effect of orexin-A on the pathological mechanism in the rat focal cerebral ischemia. Neurosci Res 2010;68:154–7.
45. Kotan D, Deniz O, Aygul R, Yildirim A. Acute cerebral ischaemia: relationship between serum and cerebrospinal fluid orexin-A concentration and infarct volume. J Int Med Res 2013;41:404–9.
46. Bittencourt JC, Presse F, Arias C, et al. The melanin-concentrating hormone system of the rat brain: an immuno- and hybridization histochemical characterization. J Comp Neurol 1992;319:218–45.
47. Sakurai T, Amemiya A, Ishii M, et al. Orexins and orexin receptors: a family of hypothalamic neuropeptides and G protein-coupled receptors that regulate feeding behavior. Cell 1998;92:1 page following 696.
48. Berridge CW, Espana RA, Vittoz NM. Hypocretin/orexin in arousal and stress. Brain Res 2010;1314:91–102.
49. King PJ. The hypothalamus and obesity. Curr Drug Targets 2005;6:225–40.
50. Machaalani R, Hunt NJ, Waters KA. Effects of changes in energy homeostasis and exposure of noxious insults on the expression of orexin (hypocretin) and its receptors in the brain. Brain Res 2013;1526:102–22.
51. Peyron C, Sapin E, Leger L, Luppi PH, Fort P. Role of the melanin-concentrating hormone neuropeptide in sleep regulation. Peptides 2009;30:2052–9.
52. Griffond B, Risold PY. MCH and feeding behavior-interaction with peptidic network. Peptides 2009;30:2045–51.
53. Saper CB, Chou TC, Scammell TE. The sleep switch: hypothalamic control of sleep and wakefulness. Trends Neurosci 2001;24:726–31.
54. Adamantidis AR, Zhang F, Aravanis AM, Deisseroth K, de Lecea L. Neural substrates of awakening probed with optogenetic control of hypocretin neurons. Nature 2007;450:420–4.
55. Monti JM, Torterolo P, Lagos P. Melanin-concentrating hormone control of sleep-wake behavior. Sleep Med Rev 2013;17:293–8.
56. Konadhode RR, Pelluru D, Blanco-Centurion C, et al. Optogenetic stimulation of MCH neurons increases sleep. J Neurosci 2013;33:10257–63.
57. Modirrousta M, Mainville L, Jones BE. Orexin and MCH neurons express c-Fos differently after sleep deprivation vs. recovery and bear different adrenergic receptors. Eur J Neurosci 2005;21:2807–16.
58. Hanriot L, Camargo N, Courau AC, Leger L, Luppi PH, Peyron C. Characterization of the melanin-concentrating hormone neurons activated during paradoxical sleep hypersomnia in rats. J Comp Neurol 2007;505:147–57.
59. Ahmed S, Meng H, Liu T, et al. Ischemic stroke selectively inhibits REM sleep of rats. Exp Neurol 2011;232:168–75.
60. Chiocchio SR, Gallardo MG, Louzan P, Gutnisky V, Tramezzani JH. Melanin-concentrating hormone stimulates the release of luteinizing hormone-releasing hormone and gonadotropins in the female rat acting at both median eminence and pituitary levels. Biol Reprod 2001;64:1466–72.
61. Naufahu J, Cunliffe AD, Murray JF. The roles of melanin-concentrating hormone in energy balance and reproductive function: are they connected? Reproduction 2013;146:R141–50.
62. Small CJ, Goubillon ML, Murray JF, et al. Central orexin A has site-specific effects on luteinizing hormone release in female rats. Endocrinology 2003;144:3225–36.
63. Bieche I, Latil A, Parfait B, et al. CGA gene (coding for the alpha subunit of glycoprotein hormones) overexpression in ER alpha-positive prostate tumors. Eur Urol 2002;41:335–41.
64. McCullough LD, Hurn PD. Estrogen and ischemic neuroprotection: an integrated view. Trends Endocrinol Metab 2003;14:228–35.
65. Li J, Siegel M, Yuan M, et al. Estrogen enhances neurogenesis and behavioral recovery after stroke. J Cereb Blood Flow Metab 2011;31:413–25.
66. Gatson JW, Singh M. Activation of a membrane-associated androgen receptor promotes cell death in primary cortical astrocytes. Endocrinology 2007;148:2458–64.
67. Caruso A, Di Giorgi Gerevini V, Castiglione M, et al. Testosterone amplifies excitotoxic damage of cultured oligodendrocytes. J Neurochem 2004;88:1179–85.
68. Garcia-Estrada J, Del Rio JA, Luquin S, Soriano E, Garcia-Segura LM. Gonadal hormones down-regulate reactive gliosis and astrocyte proliferation after a penetrating brain injury. Brain Res 1993;628:271–8.

SUPPLEMENTAL MATERIAL

Table S1—List of Taqman assays used for the qRT-PCR analysis.

Gene	RefSeq	Gene	RefSeq
GAPDH	Rn01775763_g1	CCNA2	Rn01493715_m1
pMCH	Rn00561766_g1	PLK1	Rn00690926_m1
CGA	Rn02532426_s1	CDC20	Rn00680176_m1
HCRT	Rn00565995_m1	IL1R1	Rn00565482_m1
ITGAX	Rn01511082_m1	CD14	Rn00572656_g1
CCL7	Rn01467286_m1	CD86	Rn00571654_m1
AGT	Rn00593114_m1	CD16	Rn01483598_m1
CALCR	Rn00587525_m1	IL18	Rn01422083_m1
CDK1	Rn00570728_m1	CD180	Rn01489517_m1
PTTG1	Rn00574373_m1		

AGT, angiotensin; CCL7, chemokine (C-C motif) ligand 7; CCNA2, cyclin A2; CD14, cluster of differentiation 14; CD16, cluster of differentiation 16; CD180, cluster of differentiation 180; CD86, cluster of differentiation 86; CDC20, cell-division cycle protein 20; CDK1, cyclin-dependent kinase 1; CGA, glycoprotein hormones-alpha polypeptide; GAPDH, glyceraldehyde-3-phosphate dehydrogenase; HCRT, hypocretin; IL18, interleukin 18; IL1-R1, interleukin-1 receptor 1; ITGAX, integrin, alpha X; PLK1, polo-like kinase 1; pMCH, melanin concentrating hormone; PTTG1, pituitary tumor-transforming 1.

Table S2—Top 25 up and down-regulated genes found to be common in the Venn diagram between SDp.IS/vs/IS and IS/vs/Sham contrasts.

		Fold Change	
Symbol	**Gene Name**	**SDp.IS/vs/IS**	**IS/vs/Sham**
CGA	glycoprotein hormones, alpha polypeptide	4.325	−2.044
ZBTB16	zinc finger and BTB domain containing 16	1.751	−2.264
ITIH3	inter-alpha-trypsin inhibitor heavy chain 3	1.548	−1.554
RGS22	regulator of G-protein signaling 22	1.540	−1.376
PTH2R	parathyroid hormone 2 receptor	1.518	−1.471
NEUROD6	neuronal differentiation 6	1.487	−2.622
NTNG1	netrin G1	1.474	−1.798
Epm2a	epilepsy, progressive myoclonus type 2A	1.437	−1.701
Egfem1	EGF-like and EMI domain containing 1	1.416	−1.641
RPE65	retinal pigment epithelium-specific protein 65kDa	1.413	−1.228
KCTD8	potassium channel tetramerization domain containing 8	1.411	−1.734
CYP4F8	cytochrome P450, family 4, subfamily F, polypeptide 8	1.400	−2.105
Olfr1373	olfactory receptor 1380	1.398	−1.231
PNMA3	paraneoplastic Ma antigen 3	1.392	−1.830
P2RX6	purinergic receptor P2X, ligand-gated ion channel, 6	1.384	−1.233
DGKG	diacylglycerol kinase, gamma 90kDa	1.378	−1.720
GRID2IP	glutamate receptor, ionotropic, delta 2 (Grid2) interacting protein	1.372	−1.433
Olfr1342	olfactory receptor 1342	1.372	−1.266
ZNF474	zinc finger protein 474	1.371	−1.320
NAP1L5	nucleosome assembly protein 1-like 5	1.369	−1.612
Ccdc162	coiled-coil domain containing 162	1.368	−1.543
TENM2	teneurin transmembrane protein 2	1.367	−1.731
C21orf58	chromosome 21 open reading frame 58	1.363	−1.286
METTL11B	methyltransferase like 11B	1.348	−1.377
ITGAX	integrin, alpha X (complement component 3 receptor 4 subunit)	−2.254	4.656
CCL7	chemokine (C-C motif) ligand 7	−2.034	6.762
PRR11	proline rich 11	−1.959	4.575
CD300C	CD300c molecule	−1.892	18.348
FCN1	ficolin (collagen/fibrinogen domain containing) 1	−1.889	11.079
CD14	CD14 molecule	−1.887	8.913
Timd2	T cell immunoglobulin and mucin domain containing 2	−1.845	2.786
CCNA2	cyclin A2	−1.765	7.068
CDK1	cyclin-dependent kinase 1	−1.758	6.468
CEACAM4	carcinoembryonic antigen-related cell adhesion molecule 4	−1.757	2.135
KIF4A	kinesin family member 4A	−1.730	4.279
IL18	interleukin 18 (interferon-gamma-inducing factor)	−1.718	3.295
C19orf38	chromosome 19 open reading frame 38	−1.716	5.782
Hist1h2ail	histone cluster 1, H2ai-like	−1.714	2.713
CD16a	Fc fragment of IgG, low affinity IIIa, receptor (CD16a)	−1.703	4.030
OLR1	oxidized low density lipoprotein (lectin-like) receptor 1	−1.702	8.881
CD93	CD93 molecule	−1.693	3.313
Cdkn3	cyclin-dependent kinase inhibitor 3	−1.689	8.713
PLK1	polo-like kinase 1	−1.688	6.841
RGS1	regulator of G-protein signaling 1	−1.685	2.912
HIST2H3C	histone cluster 2, H3c	−1.682	3.826
CD86	CD86 molecule	−1.681	3.059
CASC5	cancer susceptibility candidate 5	−1.679	5.205
CCNB2	cyclin B2	−1.672	5.311
PLK4	polo-like kinase 4	−1.667	4.069

Genes were selected on the SDp.IS/vs/IS comparison.

Table S3—Top 25 up and down-regulated genes found to be common between all the contrasts analyzed in the Venn diagram.

		Fold Change		
Symbol	**Gene Name**	**SDp.IS/vs/IS**	**IS/vs/Sham**	**SDp/vs/Sham**
FMO2	flavin containing monooxygenase 2 (non-functional)	2.095	−2.782	−3.150
CALCR	calcitonin receptor	2.075	−2.401	−3.446
SLC17A6	solute carrier family 17 (vesicular glutamate transporter), member 6	1.893	−2.412	−1.930
AGT	angiotensinogen (serpin peptidase inhibitor, clade A, member 8)	1.758	−2.115	−2.123
FEZF1	FEZ family zinc finger 1	1.720	−1.768	−1.586
Slc19a3	solute carrier family 19, member 3	1.584	−2.912	−1.860
ARHGAP36	Rho GTPase activating protein 36	1.563	−1.785	−2.740
ASB4	ankyrin repeat and SOCS box containing 4	1.524	−1.591	−1.493
HIF3A	hypoxia inducible factor 3, alpha subunit	1.466	−1.685	−1.507
STAC	SH3 and cysteine rich domain	1.422	−1.487	−1.572
Lrp1b	low density lipoprotein receptor-related protein 1B	1.417	−1.842	1.890
mir-154	microRNA 494	1.409	1.312	2.248
GABRQ	gamma-aminobutyric acid (GABA) A receptor, theta	1.398	−1.462	−2.917
TINAGL1	tubulointerstitial nephritis antigen-like 1	1.384	−1.363	−1.690
TMEM255A	transmembrane protein 255A	1.382	−1.463	−1.455
AGBL3	ATP/GTP binding protein-like 3	1.379	−1.265	1.336
CSMD3	CUB and Sushi multiple domains 3	1.371	−1.666	1.378
4933405O20Rik	RIKEN cDNA 4933405O20 gene	1.356	−1.352	1.814
CCSER1	coiled-coil serine-rich protein 1	1.290	−1.347	1.476
RGD1562629	similar to neurobeachin	1.284	−1.361	1.319
Olr1434	olfactory receptor 1434	1.274	−1.558	−1.377
GRIN2D	glutamate receptor, ionotropic, N-methyl D-aspartate 2D	1.270	−1.476	−1.379
B630019K06Rik	novel protein similar to F-box and leucine-rich repeat protein 17	1.267	−1.367	−1.270
ARAP2	ArfGAP with RhoGAP domain, ankyrin repeat and PH domain 2	1.254	−1.529	1.300
SEC62	SEC62 homolog (S. cerevisiae)	1.238	−1.357	1.210
Ifitm2	interferon induced transmembrane protein 2	−1.641	2.832	−1.497
PLP2	proteolipid protein 2 (colonic epithelium-enriched)	−1.602	8.036	−1.598
ANXA2	annexin A2	−1.490	5.041	−1.379
TGFB1	transforming growth factor, beta 1	−1.483	3.695	−1.473
CLIC1	chloride intracellular channel 1	−1.462	5.429	−1.426
THBD	thrombomodulin	−1.460	1.422	−1.265
Prg4	proteoglycan 4	−1.455	1.912	−1.716
Tlr13	toll-like receptor 13	−1.453	4.381	−1.575
IFITM2	interferon induced transmembrane protein 2	−1.441	2.625	−1.981
SLC1A5	solute carrier family 1 (neutral amino acid transporter), member 5	−1.434	2.195	−1.312
CLCN5	chloride channel, voltage-sensitive 5	−1.425	2.364	−1.399
B4GALT1	UDP-Gal:betaGlcNAc beta 1,4- galactosyltransferase, polypeptide 1	−1.389	2.485	−1.554
STK10	serine/threonine kinase 10	−1.383	3.066	−1.293
FXYD5	FXYD domain containing ion transport regulator 5	−1.366	3.558	−1.374
WASF2	WAS protein family, member 2	−1.355	1.697	−1.289
CD44	CD44 molecule (Indian blood group)	−1.350	4.264	−1.369
EIF4EBP1	eukaryotic translation initiation factor 4E binding protein 1	−1.337	1.694	−1.324
DSCC1	DNA replication and sister chromatid cohesion 1	−1.331	1.563	1.407
LSP1	lymphocyte-specific protein 1	−1.331	3.051	−1.484
PSMB9	proteasome (prosome, macropain) subunit, beta type, 9	−1.322	2.528	−1.469
CSF1	colony stimulating factor 1 (macrophage)	−1.300	2.342	−1.537
MFNG	MFNG O-fucosylpeptide 3-beta-N-acetylglucosaminyltransferase	−1.300	1.590	−1.400
RAB3IL1	RAB3A interacting protein (rabin3)-like 1	−1.298	2.155	−1.562
ZC3HAV1	zinc finger CCCH-type, antiviral 1	−1.296	2.273	−1.379
PLIN2	perilipin 2	−1.284	3.986	−1.413

Genes were selected on the SDp.IS/vs/IS comparison.

Table S4—Set of the 48 altered genes expressed exclusively in SDp.IS/vs/S contrast.

Symbol	Gene Name	Fold Change SDp.IS/vs/IS
PMCH	pro-melanin-concentratinghormone	6.915
HCRT	hypocretin (orexin) neuropeptideprecursor	2.209
DMC1	DNA meioticrecombinase 1	1.464
Dnah9	dynein, axonemal, heavy chain 9	1.44
Olfr1349	olfactoryreceptor 1349	1.414
USP17L2	ubiquitin specific peptidase 17-like family member 2	1.398
BC051142	cDNAsequence BC051142	1.378
mir-493	microRNA 493	1.371
CABP7	calciumbindingprotein 7	1.364
LAIR1	leukocyte-associated immunoglobulin-like receptor 1	1.339
SPATA17	spermatogenesisassociated 17	1.319
1700106J16Rik	RIKEN cDNA 1700106J16 gene	1.28
PGLYRP1	peptidoglycanrecognitionprotein 1	1.277
Olfr150	olfactoryreceptor 150	1.274
LOC688916	hypotheticalprotein LOC688916	1.266
4933408B17Rik	RIKEN cDNA 4933408B17 gene	1.257
KRT78	keratin 78	1.257
2610034M16Rik	RIKEN cDNA 2610034M16 gene	1.253
TAS2R4	taste receptor, type 2, member 4	1.243
OTOP1	otopetrin 1	1.242
LOC100363193	LRRGT00076-like	1.233
MTNR1B	melatoninreceptor 1B	1.225
P2RX3	purinergic receptor P2X, ligand-gated ion channel, 3	1.221
SRP72	signalrecognitionparticle 72kDa	1.186
PSAT1	phosphoserineaminotransferase 1	1.171
ANKRD52	ankyrinrepeatdomain 52	−1.193
STARD8	StAR-related lipid transfer (START) domain containing 8	−1.203
TEX264	testisexpressed 264	−1.204
Rsg1	REM2 and RAB-like small GTPase 1	−1.206
Cyc1	cytochrome c-1	−1.215
ITPA	inosinetriphosphatase (nucleosidetriphosphatepyrophosphatase)	−1.216
BNIP1	BCL2/adenovirus E1B 19kDa interactingprotein 1	−1.22
TCF7L1	transcription factor 7-like 1 (T-cell specific, HMG-box)	−1.22
SMIM20	small integral membraneprotein 20	−1.221
MAZ	MYC-associatedzincfingerprotein (purine-bindingtranscriptionfactor)	−1.227
MRPL23	mitochondrialribosomalprotein L23	−1.23
Tmem234	transmembraneprotein 234	−1.231
RHBDD3	rhomboiddomaincontaining 3	−1.237
PPP1CA	proteinphosphatase 1, catalyticsubunit, alphaisozyme	−1.24
Ap1s3	adaptor-relatedproteincomplex 1, sigma 3 subunit	−1.241
EMG1	EMG1 N1-specific pseudouridinemethyltransferase	−1.244
NUDT14	nudix (nucleoside diphosphate linked moiety X)-type motif 14	−1.255
CDK20	cyclin-dependentkinase 20	−1.263
GK5	glycerolkinase 5 (putative)	−1.265
GEMIN7	gem (nuclearorganelle) associatedprotein 7	−1.269
Akr1c14	aldo-ketoreductase family 1, member C14	−1.278
HIST3H2BB	histonecluster 3, H2bb	−1.31
STC1	stanniocalcin 1	−1.404